

Optical absorption spectra associated with donors in a corner under an applied electric field

This article has been downloaded from IOPscience. Please scroll down to see the full text article.

1998 J. Phys.: Condens. Matter 10 3977

(<http://iopscience.iop.org/0953-8984/10/18/008>)

View [the table of contents for this issue](#), or go to the [journal homepage](#) for more

Download details:

IP Address: 171.66.16.151

The article was downloaded on 12/05/2010 at 23:22

Please note that [terms and conditions apply](#).

Optical absorption spectra associated with donors in a corner under an applied electric field

Zhen-Yan Deng, Qian-Bing Zheng and Takayoshi Kobayashi†

Department of Physics, School of Science, University of Tokyo, 7-3-1 Hongo, Bunkyo-ku, Tokyo 113, Japan

Received 15 September 1997, in final form 9 February 1998

Abstract. We study shallow-donor impurity states and the optical absorption spectra associated with transitions from the $n = 1$ valence subband to the donor impurities in a corner under an applied electric field. It is found that the energy contours for the impurity binding ($E_b = E$) in the corner become closed when a suitable electric field is applied; this is similar to the impurity-state behaviour in quantum wires. When the electric field strength increases, the centre of the contours moves towards the corner and the centre impurity binding energy increases. The optical absorption spectra associated with donors in the corner are also similar to those of quantum wires when the electric field is applied, and the width of the absorption spectra increases with the increase in the electric field strength.

1. Introduction

The progress in material growth techniques, such as molecular-beam epitaxy and organometallic chemical vapour deposition, has made it possible to fabricate semiconductor microstructures down to nanometre size. In the past few years, many investigations, both theoretical and experimental, have been devoted to the study of the nature of hydrogenic impurity states in such semiconductor nanostructures (quantum wells and quantum wires). Because of the confinement of electrons in these low-dimensional systems, the electronic energy levels become discrete and the impurity binding energies are enhanced, compared with those in the bulk.

The interfaces in low-dimensional semiconductor systems play a significant role in determining their electronic and optical properties, and step structures usually exist at the interfaces [1–6], which affect their optical transition spectra considerably. In fact, a stepped surface or V-shaped groove of large size in an interface can be viewed as a corner. This model has been adopted by Lee and Antoniewicz [7, 8] in studying surface bound states and surface polaron states. In our previous papers [9–12], we have investigated the electronic, excitonic and hydrogenic impurity states in a corner with and without an electric field, and many interesting results have been obtained. It was found that the ground-state impurity binding energy in a right-angled corner tends to the value of the third impurity excited state in the bulk when the impurity approaches the corner [9], and the optical absorption spectra associated with impurities in the right-angled corner extend compared with those for the bulk [10]. Moreover, the impurity binding energy decreases, but the exciton binding energy appears to undergo no change, as the value of the corner angle becomes small [11]. It was

† Author to whom any correspondence should be addressed.

also found that the electronic and impurity states in the corner under an applied electric field are similar to those in quantum wires, and the impurity binding energy in the corner increases with the increase in the electric field strength [12].

In this paper, we study the energy contours for the impurity binding and optical absorption spectra associated with transitions from the $n = 1$ valence subband to the donor levels in a right-angled corner under an applied electric field. In section 2, the theoretical framework is outlined. The results and a discussion are presented in section 3.

2. Theory

When an electric field $\mathbf{F} = (1, 1, 0)(F/\sqrt{2})$ is applied along the diagonal line of a right-angled corner, in the effective-mass approximation, the electronic and impurity-state Hamiltonians in the corner can be written as

$$H_0(\mathbf{r}) = P^2/(2m) + V(\mathbf{r}) + eFx/\sqrt{2} + eFy/\sqrt{2} \quad (1)$$

and

$$H(\mathbf{r}) = H_0(\mathbf{r}) - e^2/(\varepsilon|\mathbf{r} - \mathbf{r}_0|) \quad (2)$$

where m is the electron-band effective mass; \mathbf{r} and \mathbf{P} are the electron coordinate and momentum, respectively; ε is the dielectric constant of the well material and $\mathbf{r}_0 = (x_0, y_0, 0)$ is the impurity position; and

$$V(\mathbf{r}) = \begin{cases} 0 & x > 0 \text{ and } y > 0 \\ \infty & \text{otherwise} \end{cases} \quad (3)$$

is the electron-confining potential well in the corner. The electronic wavefunction $\Phi_0(\mathbf{r})$ and ground-state energy level E_0 for the electronic Hamiltonian $H_0(\mathbf{r})$ can be obtained as follows [12]:

$$\begin{aligned} \Phi_0(\mathbf{r}) &= N_0 \text{Ai}(\xi) \text{Ai}(\zeta) \\ \xi &= (x/l) - \lambda_1 \\ \zeta &= (y/l) - \lambda_1 \\ l &= [\hbar^2/(\sqrt{2}meF)]^{1/3} \end{aligned} \quad (4)$$

and

$$E_0 = \lambda_1 \hbar^2/(2ml^2) \quad (5)$$

where N_0 is the normalization constant, l is the electron characteristic length under the electric field and λ_1 is the first zero point of the Airy function $\text{Ai}(\xi)$. The ground-state donor binding energy E_b is defined as the energy difference between the bottom of the electronic conduction band without the impurity and the ground-state energy level of donor states in the corner:

$$E_b = E_0 - \min_{\beta} \langle \psi(\mathbf{r}) | H(\mathbf{r}) | \psi(\mathbf{r}) \rangle. \quad (6)$$

Here

$$\psi(\mathbf{r}) = N(\beta) \Phi_0(\mathbf{r}) \exp(-\beta|\mathbf{r} - \mathbf{r}_0|) \quad (7)$$

is the trial wavefunction for the ground donor state, and $N(\beta)$ is the normalization constant and β is the variational parameter.

For an optical transition from the first valence subband to a donor level, we have for the initial state

$$|i\rangle = \Phi_0(\mathbf{r})L_z^{-1/2} \exp(ik_z z)u_i(\mathbf{r}) \quad (8)$$

where L_z is the length of the corner structure in the z -direction. For the final state, the wave function is

$$|f\rangle = \psi(\mathbf{r})u_f(\mathbf{r}). \quad (9)$$

In equations (8) and (9), $u_i(\mathbf{r})$ and $u_f(\mathbf{r})$ are the periodic parts of the Bloch state for the initial and final states, respectively.

Taking the energy origin at the bottom of the first conduction subband, we have for the energy of the initial state

$$E_i = -\varepsilon_g - \frac{\hbar^2}{2m_h}k_z^2 \quad (10)$$

where m_h is the hole effective mass of the valence band and

$$\varepsilon_g = E_g + E_0^c + E_0^v \quad (11)$$

with E_g being the bulk band gap and E_0^c (E_0^v) the ground energy level of the first conduction (valence) subband in the corner. The energy of the final state is

$$E_f = -E_b(\mathbf{r}_0, F) \quad (12)$$

where $E_b(\mathbf{r}_0, F)$ is the binding energy of the donor impurity.

The transition probability per unit time for transition from the first valence subband to the donor level associated with the impurity located at the position \mathbf{r}_0 is proportional to the square of the matrix element of the electron–photon interaction H_{int} connecting the wavefunctions of the initial (valence) state and final (donor) state [13, 14]:

$$W(\omega, F, \mathbf{r}_0) = \frac{2\pi}{\hbar} \sum_i |\langle f|H_{int}|i\rangle|^2 \delta(E_f - E_i - \hbar\omega) \quad (13)$$

with $H_{int} = C\mathbf{e} \cdot \mathbf{P}$, where \mathbf{e} is the polarization vector in the direction of the electric field of the radiation, \mathbf{P} is the electric dipole moment and C is a prefactor that describes the effect of the photon vector potential. The above matrix element may be written as

$$\langle f|H_{int}|i\rangle \cong C\mathbf{e} \cdot \mathbf{P}_{fi}S_{fi} \quad (14)$$

with

$$\mathbf{P}_{fi} = \frac{1}{\Omega} \int_{\Omega} u_f^*(\mathbf{r})\mathbf{P}u_i(\mathbf{r}) \, d\mathbf{r} \quad (15)$$

and

$$S_{fi} = \int F_f^*(\mathbf{r})F_i(\mathbf{r}) \, d\mathbf{r} \quad (16)$$

where Ω is the volume of a unit cell and $F_f(\mathbf{r})$ ($F_i(\mathbf{r})$) is the envelope function for the final (initial) state. Then equation (13) can be simplified further:

$$W(\omega, F, \mathbf{r}_0) = [L_z m^{1/2}/(\sqrt{2}\hbar^2)]|C|^2|\mathbf{e} \cdot \mathbf{P}_{fi}|^2|S_{fi}(\mathbf{r}_0, k_z(\Delta))|^2 Y(\Delta)/\Delta^{1/2} \quad (17)$$

where $Y(\Delta)$ is the step function and

$$\Delta = \hbar\omega + E_b(\mathbf{r}_0, F) - \varepsilon_g \quad (18)$$

$$k_z(\Delta) = (2m_h \Delta/\hbar^2)^{1/2}. \quad (19)$$

In practice, implanted impurities exist everywhere in the corner. If a uniform distribution of donor impurities is considered, the total transition probability per unit time for transitions from the first valence subband to the donor impurities in the corner can be obtained:

$$\begin{aligned} W(\omega, F) &= (L_x L_y)^{-1} \int_0^{L_x} dx_0 \int_0^{L_y} dy_0 W(\omega, F, \mathbf{r}_0) \\ &= W_0 (L_x L_y)^{-1} \int_0^{L_x} dx_0 \int_0^{L_y} dy_0 |S_{fi}(\mathbf{r}_0, k_z(\Delta))|^2 Y(\Delta) / \Delta^{1/2} \end{aligned} \quad (20)$$

where

$$W_0 = [L_z m^{1/2} / (\sqrt{2} \hbar^2)] |C|^2 |e \cdot \mathbf{P}_{fi}|^2 \quad (21)$$

and $L_x \times L_y$ is the integral zone selected in the corner. The above integrals were calculated numerically.

3. Results and discussion

As an example, we chose a GaAs/AlAs corner for the numerical calculation, with GaAs being the well material. For simplicity, the energy is in units of effective rydbergs, $\text{Ryd}^* = m_e e^4 / 2 \hbar^2 \epsilon^2$, and the length is normalized to the effective Bohr radius, $a_0^* = \hbar^2 \epsilon / m_e e^2$, with m_e being the electron effective mass of the conduction band. In our calculation, we have used $\epsilon = 12.58$, $m_e = 0.0665 m_0$ and $m_h = 0.30 m_0$ for the GaAs well material with m_0 being the free-electron mass [13], and a $10a_0^* \times 10a_0^*$ integral zone was adopted for the calculation of the total optical transition probability.

The results of our previous paper [12] showed that the impurity-state behaviour in the corner under an electric field is similar to that in quantum wires; this means that a maximum impurity binding energy exists somewhere in the corner, as the binding energy at the cross section centre of the quantum wires is a maximum. Figure 1 shows the maximum impurity binding energy and its corresponding impurity position in the corner versus the applied electric field strength. From figure 1, it can be seen that the maximum impurity binding energy increases and its corresponding impurity position tends towards the corner as the electric field strength increases; this is similar to the situation in quantum wires in which

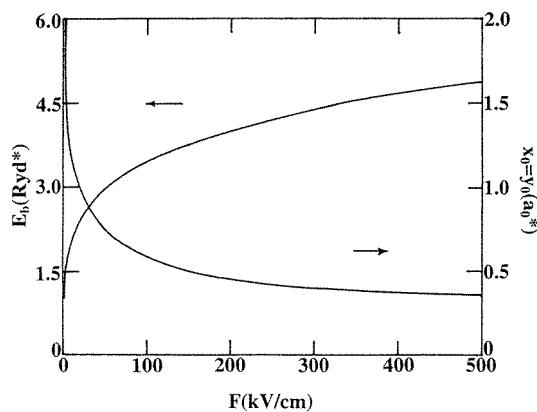


Figure 1. Variations in the maximum impurity binding energy and its corresponding impurity position in the corner with the electric field strength.

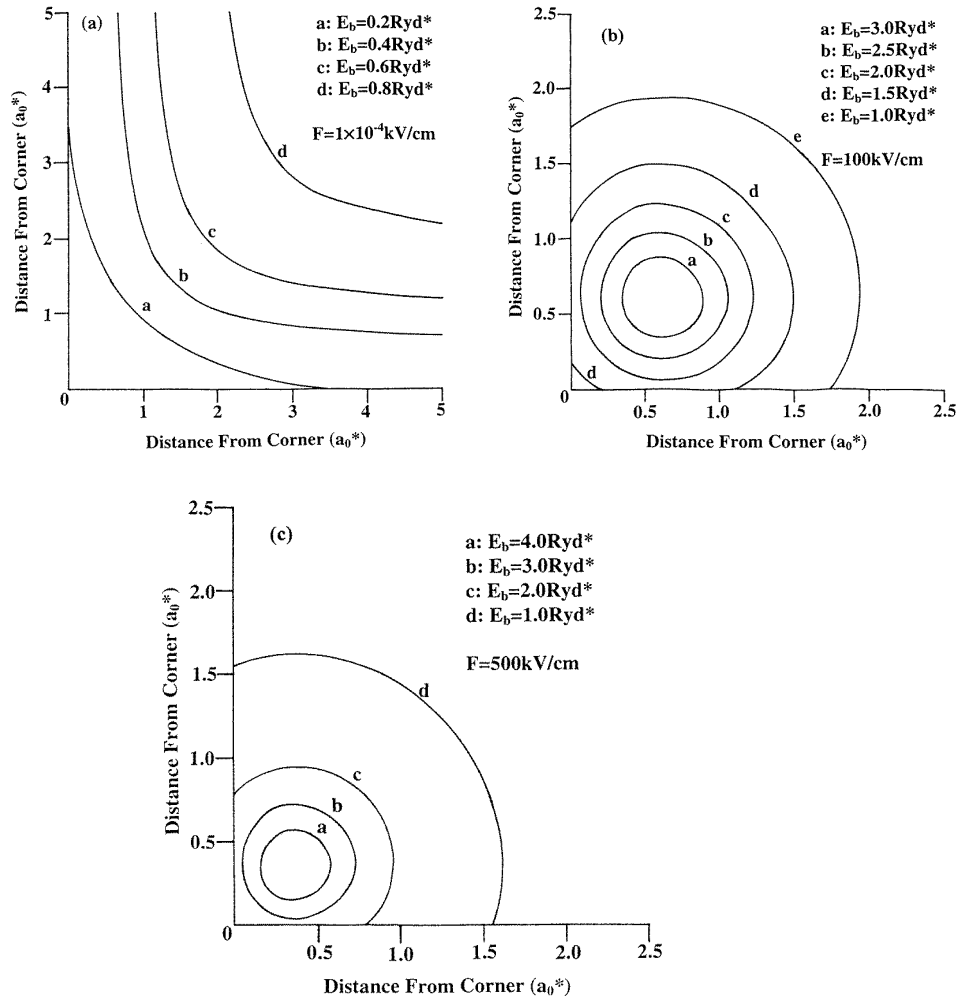


Figure 2. The contours of the impurity binding energy in the corner for different electric fields: (a) $F = 1 \times 10^{-4} \text{ kV cm}^{-1}$, (b) $F = 100 \text{ kV cm}^{-1}$, and (c) $F = 500 \text{ kV cm}^{-1}$.

the impurity binding energy at the centre of the quantum wire increases with the decrease in the size of the quantum wire [15, 16]. Figure 2 shows the contours of impurity binding energy in the corner for different applied electric fields; it indicates that the contours of the impurity binding energy become closed when a suitable electric field is applied. When the electric field strength increases, the impurity binding energy in the corner increases and the centre of the contours of the impurity binding energy moves towards the corner, which is in agreement with the results of figure 1. As we know, the contours of impurity binding energy for quantum wires are closed [17], and the results of figure 2 intuitively indicate that the impurity-state behaviour in the corner under the applied electric field is similar to that in quantum wires, and the equivalent size of quantum wire decreases with increase in the electric field strength [12].

Figure 3 shows the possible optical transitions from the first valence subband to the donor impurities in the corner, where $\hbar\omega_1$ and $\hbar\omega_2$ represent the energies of the transitions

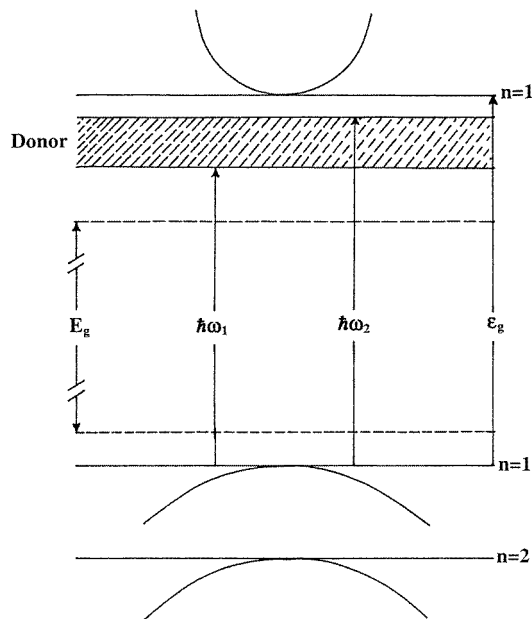


Figure 3. A schematic representation of the possible optical transitions from the first valence subband to the donor impurities in a corner under an applied electric field, where the parabolae represent the energy dispersions of the first conduction and valence subbands in the direction normal to corner cross section.

from the top of the first valence subband to the bottom and top of the donor impurity levels, respectively. Figure 4 shows the optical absorption spectra associated with donors in the GaAs/AlAs corner for different electric field strengths. Figure 4 indicates that there are two apparent absorption peaks on the high- and low-energy sides when the electric field strength is almost zero ($F = 1 \times 10^{-4} \text{ kV cm}^{-1}$), and these two peaks correspond to the impurity binding energies in the bulk and that along one side of the corner, respectively. However, when a suitable electric field is applied, the absorption peak on the low-energy side disappears and the width of the absorption spectra increases. Figure 4 also indicates that the height of the absorption peak on the high-energy side decreases and the width of the absorption spectra increases as the electric field strength increases.

The results obtained by us are interesting, and their physical interpretation and a discussion of their features follows. Because of the existence of the applied electric field, the electrons are pushed towards the corner, and the electronic and impurity-state behaviour in the corner is similar to that of quantum wires [12]; so the contours of the impurity binding energy in the corner are closed when a suitable electric field is applied. When the electric field strength increases, the confinement of electrons in the corner is enhanced and the equivalent size of the quantum wire decreases [12], and therefore the centre of the contours of the impurity binding energy in the corner tends towards the corner and the maximum binding energy at the centre of the contours increases. The dependence of the shape of the optical absorption spectra in the corner on the electric field strength is similar to that of optical absorption spectra of a quantum wire on the size of its cross section. For example, Porrás-Montenegro and Oliveira [13] studied the optical absorption spectra associated with

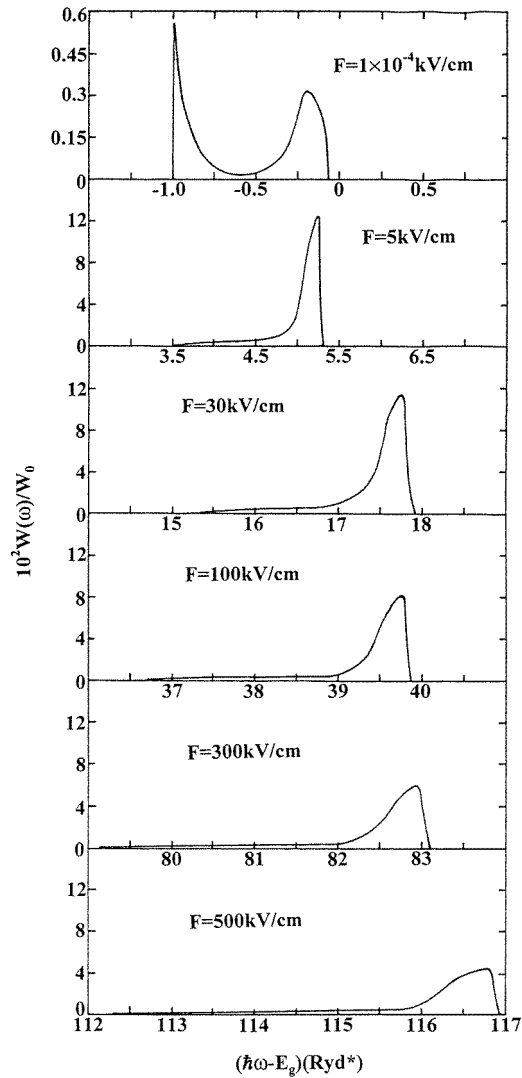


Figure 4. The optical absorption probability per unit time for the transitions from the first valence subband to the donor impurities in the corner as a function of $\hbar\omega - E_g$ for different electric fields.

transitions between the $n = 1$ valence subband and the donor impurities in a cylindrical quantum wire with an infinitely confining potential, and found that there are two apparent absorption peaks on the low- and high-energy sides when the radius of the quantum wire is 1000 \AA , and the peak on the low-energy side disappears when the radius of the quantum wire is reduced to 50 \AA . At the same time, the width of the absorption spectra increases monotonically with the decrease in the radius of the quantum wire. The optical absorption spectra associated with the donor impurities in the corner are closely related to the density of the impurity states [17]. When the applied electric field is almost the zero, most of the impurities in the corner have the same impurity binding energy as in the bulk (1 Ryd^*) and some of the impurities along two sides of the corner have impurity binding energies of about $1/4 \text{ Ryd}^*$ [12] in the integral zone that we considered, as shown in figure 2(a), and there are two apparent absorption peaks on the high- and low-energy sides of the optical absorption spectra in the corner. When a suitable electric field is applied, the situation is

changed; that is, the contours of the impurity binding energy are closed, and most of the impurity states in the integral zone that we considered lie at the area with lower impurity binding energy, as shown in figures 2(b) and 2(c); so only one absorption peak exists on the high-energy side of the absorption spectra in the corner when a suitable electric field is applied, as shown in figure 4. The width of the optical absorption spectra in the corner is also related to the width of the donor impurity levels, as shown in figure 3. In a sense, the width of the absorption spectra is equal to the width of the donor impurity levels. When the applied electric field increases, the maximum binding energy in the corner increases, but the lowest binding energy in the corner changes little [12], and therefore the width of the donor levels in the corner increases. This is why the width of the absorption spectra in the corner increases with the increase in the electric field strength.

In summary, we have studied the shallow-donor impurity states and the optical absorption spectra associated with transitions from the first valence subband to the donor impurities in a corner under an applied electric field. The results showed that the contours of the impurity binding energy in the corner become closed when a suitable electric field is applied, and the centre of the contours moves towards the corner as the electric field strength increases, which intuitively indicates that the impurity-state behaviour in the corner under an applied electric field is similar to that for quantum wires. The optical absorption spectra in the corner under the applied electric field are also similar to those of quantum wires, and there is only one absorption peak on the high-energy side of the absorption spectra and the width of the absorption spectra increases with the increase in the electric field strength. As we know, it is easier to fabricate a corner structure than to fabricate a quantum wire in experiments, and our theoretical results may provide a new way to detect quantum confining effects in quantum wires.

Acknowledgment

One of the authors (Zhen-Yan Deng) would like to thank for support the Inoue Foundation for Science (IFS).

References

- [1] Weisbuch C, Dingle R, Gossard A C and Weigmann W 1980 *J. Vac. Sci. Technol.* **17** 1128
- [2] Fujiwara K, Kanamoto K and Tsukada N 1989 *Phys. Rev. B* **40** 9698
- [3] Tanaka M and Sakaki H 1988 *Japan. J. Appl. Phys.* **27** L2025
- [4] Tanaka M and Sakaki H 1989 *Appl. Phys. Lett.* **54** 1326
- [5] Tsuchiya M, Gaines J M, Yan R H, Simes R J, Holtz P O, Coldren L A and Petroff P M 1989 *Phys. Rev. Lett.* **62** 466
- [6] Khoo G S and Ong C K 1993 *J. Phys.: Condens. Matter* **5** 6507
- [7] Lee W W and Antoniewicz P R 1989 *Phys. Rev. B* **40** 3352
- [8] Lee W W and Antoniewicz P R 1989 *Phys. Rev. B* **40** 9920
- [9] Deng Z Y, Zhang H and Guo J K 1994 *J. Phys.: Condens. Matter* **6** 9729
- [10] Deng Z Y, Zhang H, Shi J L and Guo J K 1995 *J. Phys.: Condens. Matter* **7** 6493
- [11] Deng Z Y 1996 *J. Phys.: Condens. Matter* **8** 7443
- [12] Zhou H Y and Deng Z Y 1997 *J. Phys.: Condens. Matter* **9** 1241
- [13] Porrás-Montenegro N and Oliveira L E 1990 *Solid State Commun.* **76** 275
- [14] Deng Z Y 1996 *J. Phys.: Condens. Matter* **8** 1511
- [15] Brum J A 1985 *Solid State Commun.* **54** 179
- [16] Deng Z Y, Lai T R, Guo J K and Gu S W 1994 *J. Appl. Phys.* **75** 7389
- [17] Porrás-Montenegro N, López-Gondar J and Oliveira L E 1991 *Phys. Rev. B* **43** 1824